Optical Properties of Metal-Dielectric Films

Andrey K. Sarychev and Vladimir M. Shalaev

Abstract

Optical response of metal–dielectric inhomogeneous films is considered. A Generalized Ohm's Law is formulated to relate the electric and magnetic fields *outside* to the currents *inside* the film. Computer simulations show that the local electric and magnetic fields experience giant spatial fluctuations. The fields are localized in small spatially separated peaks: electric and magnetic hot spots. Optical transmittance through a periodically inhomogeneous metallic film is strongly enhanced when the incident wave is in resonance with surface plasmon polaritons excited in the film, and can be exploited for optical switching. An analytical theory for extraordinary light transmittance through an optically thick metallic film with subwavelength holes is developed. The transmittance has sharp peaks due to the internal resonances in the holes. At a resonance, electric and magnetic fields are dramatically enhanced in the holes. These resonances are proposed to circuit light over a metallic film for distances on the nanometer length scale.

1 Introduction

The last two decades have been a time of immense improvement in our understanding of the optical properties of inhomogeneous materials. An important representative class of such materials is constituted by metal-dielectric composite materials near the percolation threshold. Nanostructured materials of this class have attracted attention because of their unique electromagnetic properties. Many fundamental phenomenons, such as localization and delocalization of electrons and optical excitations, play important roles in random materials. The light-induced plasmon modes in metal-dielectric composite materials can result in dramatic enhancement of optical responses over broad spectral ranges. In particular, percolating metal-dielectric films can be employed for (i) surface-enhanced spectroscopy with unsurpassed sensitivity and (ii) novel optical elements, such as optical switches and efficient optical filters [1]-[3].

We consider the optical properties of random metal-dielectric films, also known as *semicontinuous metallic films*, in this chapter. These films are usually produced by either thermal evaporation or sputtering of a metal onto an insulating substrate. During the growth process, small clusters of metallic grains are formed first; and, eventually, a continuous conducting path appears between the ends of the sample at a percolation threshold, indicating a metal-insulator transition in the system. At high surface coverage, the film is mostly metallic with voids of irregular shapes; and finally the film becomes uniformly metallic. Although these films have been intensively studied both experimentally and theoretically for some time [4]-[19], the important role of giant local-field fluctuations, resulting from plasmon localization, was recognized only recently [20]-[38].

A two-dimensional inhomogeneous film is a thin layer within which the local physical properties are not uniform. The response of such a inhomogeneous layer to impinging plane electromagnetic waves crucially depends on (i) the spatial scale of the inhomogeneity compared to the wavelength and (ii) the angle of incidence. Usually, when the wavelength is smaller than the inhomogeneity length scale, the incident wave is scattered in various directions. The total field scattered in a certain direction is the sum of the elementary waves scattered in that direction by each elementary scatterer on the surface. As each elementary wave is specified not only by its amplitude, but also by its phase and direction of propagation, the sum of the elementary waves is a vector sum. The scattered energy is then distributed in various directions, though certain privileged directions may receive more energy than others.

By contrast, when the inhomogeneity spatial scale is much smaller than the wavelength, the resolution of the wave is too small in contrast to the nonuniformities. Therefore, the incident plane wave is then reflected specularly and transmitted in a well-defined direction, as if the film were a homogeneous layer with bulk effective physical properties (conductivity, permittivity, and permeability), as has been studied for about two centuries [39] and is considered elsewhere in this book [39]-[41]. The electromagnetic field is coupled to the inhomogeneities in such a way that irregular currents are excited on the surface of the layer. Strong distortions of the field then appear near the surface, but they decay exponentially so that the scattered field asserts a plane wave character when far away from the surface.

2 Generalized Ohm's law approximation and giant fluctuations of local electromagnetic fields

A new analytical approach to the calculation of optical properties of metal-dielectric films, referred to as the Generalized Ohm's Law (GOL), has recently been proposed [1]. We restrict ourselves, for simplicity, to the case where all the external fields are parallel to the plane of the film (i.e., when a plane wave is normally incident on a flat surface). The z axis is perpendicular to the metallic film (with possible holes, voids, or other inhomogeneities) of thickness h. The external electromagnetic wave is incident on the front interface $z=-h/2$, and the transmitted wave is emitted from the back interface $z=h/2$, as it is shown in Figure 1. The typical spatial scale D of the metallic grains is supposed to be much smaller than the free-space wavelength λ_0; i.e., $D \ll \lambda_0$.

We consider first the electric and magnetic fields in the close vicinity to the film in the front reference plane $z=-h/2-a$ and in the back reference plane $z=h/2+a$, as it is shown in Figure 1. The electric and magnetic fields considered at distance a in front of the film are designated as

$$\mathbf{E}_1(\mathbf{r}) = \mathbf{E}(\mathbf{r}, -h/2-a), \quad \mathbf{H}_1(\mathbf{r}) = \mathbf{H}(\mathbf{r}, -h/2-a), \tag{1}$$

and those at a distance a behind the film are denoted by

$$\mathbf{E}_2(\mathbf{r}) = \mathbf{E}(\mathbf{r}, h/2+a), \quad \mathbf{H}_2(\mathbf{r}) = \mathbf{H}(\mathbf{r}, h/2+a). \tag{2}$$

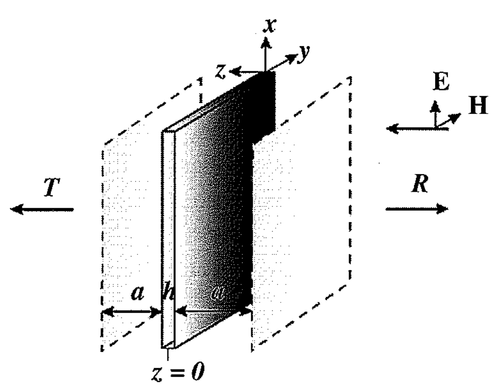

Figure 1 Electromagnetic wave of wavelength λ_0 impinges on a metal-dielectric film. It is partially reflected and absorbed, and the remainder is transmitted through the film. Electric and magnetic fields are considered in the plane $z=-h/2-a$ in front of the film and in the plane $z=h/2+a$ behind the film.

All the fields are monochromatic with the usual $\exp(-i\omega t)$ time-dependence. The vector $\mathbf{r} = \{x, y\}$ is a two-dimensional vector in the xy plane. In the case of laterally inhomogeneous films, the average electric displacement

$$\mathbf{D}(\mathbf{r}) = k_0 \int_{-h/2-a}^{h/2+a} \mathbf{D}(\mathbf{r}, z)\, dz = k_0 \int_{-h/2-a}^{h/2+a} \varepsilon(\mathbf{r}, z)\mathbf{E}(\mathbf{r}, z)\, dz \tag{3}$$

and the average magnetic induction

$$\mathbf{B}(\mathbf{r}) = k_0 \int_{-h/2-a}^{h/2+a} \mathbf{B}(\mathbf{r}, z)\, dz = k_0 \int_{-h/2-a}^{h/2+a} \mu(\mathbf{r}, z)\mathbf{H}(\mathbf{r}, z)\, dz \tag{4}$$

are functions of $\mathbf{r}$, where $k_0 = 2\pi/\lambda_0 = \omega/c$ is the free-space wavenumber. Vectors $\mathbf{D}$ and $\mathbf{B}$, introduced by (3) and (4), have the same dimension as electric displacement and magnetic induction. We assume hereafter, for simplicity, that the permittivity ε is a scalar and the permeability $\mu = 1$. Note that Gaussian units are used in this chapter.

In the GOL approximation, the local electromagnetic field is a superposition of two plane waves propagating in $+z$ and $-z$ directions. This superposition is different in different regions of the film. We neglect scattered and evanescent waves that propagate in the xy plane since their amplitudes are proportional to $(\lambda_0/D)^2$. Thus, we use the two–plane-wave approximation when both $\mathbf{E}(\mathbf{r}, z)$ and $\mathbf{H}(\mathbf{r}, z)$ have components in the xy plane only. The, superposition of two plane waves is determined by the fields $\mathbf{E}_1$ and $\mathbf{H}_1$ or $\mathbf{E}_2$ and $\mathbf{H}_2$, defined in the front or back reference planes respectively [see (1), (2)]. Therefore, in the GOL approximation the fields $\mathbf{E}(\mathbf{r}, z)$ and $\mathbf{H}(\mathbf{r}, z)$ are completely determined by either $\mathbf{E}_1(\mathbf{r})$ and $\mathbf{H}_1(\mathbf{r})$ or $\mathbf{E}_2(\mathbf{r})$ and $\mathbf{H}_2(\mathbf{r})$ or any two linear combinations of these fields.

Then, the Maxwell equations $\operatorname{curl}\mathbf{E}(\mathbf{r}, z) = ik_0\mathbf{B}(\mathbf{r}, z)$ and $\operatorname{curl}\mathbf{H}(\mathbf{r}, z) = -ik_0\mathbf{D}(\mathbf{r}, z)$, on integration from $z = -h/2 - a$ to $z = h/2 + a$, yield

$$\{\mathbf{n}\times[\mathbf{E}_1(\mathbf{r}) - \mathbf{E}_2(\mathbf{r})]\} = i\mathbf{B}(\mathbf{r}), \quad \{\mathbf{n}\times[\mathbf{H}_1(\mathbf{r}) - \mathbf{H}_2(\mathbf{r})]\} = -i\mathbf{D}(\mathbf{r}), \tag{5}$$

where $\mathbf{n} = \{0, 0, 1\}$ is the unit normal to the xy plane. The fields $\mathbf{E}_{1,2}(\mathbf{r})$ and $\mathbf{H}_{1,2}(\mathbf{r})$ have components only in the xy plane, as their z-directed components vanish in the two-wave approximation; hence, these fields as functions of the vector $\mathbf{r}$ are curl-free (otherwise they should have z components according to the Maxwell equations).

It is convenient to introduce the linear combinations of the fields $\mathbf{E}_{1,2}(\mathbf{r})$ and $\mathbf{H}_{1,2}(\mathbf{r})$; namely the fields

$$\mathbf{E}(\mathbf{r}) = \mathbf{E}_1(\mathbf{r}) + \mathbf{E}_2(\mathbf{r}), \quad \mathbf{H}(\mathbf{r}) = \mathbf{H}_1(\mathbf{r}) + \mathbf{H}_2(\mathbf{r}) \tag{6}$$

that are also curl-free:

$$\operatorname{curl}\mathbf{E}(\mathbf{r}) = \mathbf{0}, \quad \operatorname{curl}\mathbf{H}(\mathbf{r}) = \mathbf{0}, \tag{7}$$

and also determine the fields inside the film. The continuity equations for the average "electric displacement" $\mathbf{D}(\mathbf{r})$ and the average "magnetic induction" $\mathbf{B}(\mathbf{r})$ in (5) are obtained by integration of the local (3D) equations $\operatorname{div}\mathbf{D}=0$, $\operatorname{div}\mathbf{B}=0$ over the coordinate "z" between the reference planes $z=-h/2-a$ and $z=h/2+a$, which results in

$$\operatorname{div}\mathbf{D}(\mathbf{r})=0, \quad \operatorname{div}\mathbf{B}(\mathbf{r})=0, \tag{8}$$

where we take into account that the components $D_z=0$ and $B_z=0$ at the planes $z=-h/2-a$ and $z=h/2+a$.

Equations (5), (7) and (8) are the system of GOL equations that connect electric and magnetic fields, determined in (2D) reference planes, to the average electric displacement (electric current) and average magnetic induction (magnetic current) flows in the film. Thus, the entire physics of 3D inhomogeneous film, which is described by the full set of Maxwell equations, has been reduced to a set of quasistatic equations (7) and (8). To solve these equations we just need the constitutive equations connecting the fields $\mathbf{E}$ and $\mathbf{H}$ to the "currents" $\mathbf{D}$ and $\mathbf{B}$.

Since the fields $\mathbf{E}$ and $\mathbf{H}$ can completely determine the fields inside the film in the considered GOL (two-wave) approximation, the average (2D) electric displacement $\mathbf{D}(\mathbf{r})$ and the average magnetic induction $\mathbf{B}(\mathbf{r})$ can be presented as linear combinations $\mathbf{D}=u\mathbf{E}+g_1\mathbf{H}$ and $\mathbf{B}=v\mathbf{H}+g_2\mathbf{E}$, where u, v, g_1, and g_2 are dimensionless *ohmic* parameters. For simplicity, we consider films having mirror symmetry with respect to reflection in the $z=0$ plane. For such films, parameters $g_1=0$ and $g_2=0$ [18-19], [22]. Therefore, we can write

$$\mathbf{D}(\mathbf{r})=u(\mathbf{r})\mathbf{E}(\mathbf{r}), \quad \mathbf{B}(\mathbf{r})=v(\mathbf{r})\mathbf{H}(\mathbf{r}), \tag{9}$$

where dimensionless ohmic parameters $u(\mathbf{r})$ and $v(\mathbf{r})$ are expressed in terms of the local refractive index $n=\sqrt{\varepsilon(\mathbf{r})}$ as

$$u=\frac{\tan(Dk_0/4)+n\tan(hk_0n/2)}{1-n\tan(Dk_0/4)\tan(hk_0n/2)} \tag{10}$$

and

$$v=\frac{n\tan(Dk_0/4)+\tan(hk_0n/2)}{n-\tan(Dk_0/4)\tan(hk_0n/2)}. \tag{11}$$

The refractive index n takes the values $n_m=\sqrt{\varepsilon_m}$ and $n_d=\sqrt{\varepsilon_d}$ for the metallic and the dielectric regions of the film. The distance to the reference planes is set $a=D/4$ in (10) and (11) [16], [19], [35]. Note that this choice of a is close to $a=2D/(3\pi)$, which is obtained from comparison of GOL and exact results [42] for the diffraction by a small aperture in a perfectly conducting screen. Equations (9) have the form typical for constitutive equations in electromagnetism [43], but include parameters u and v which incorporate local geometry of the film.

In order to find the observable optical properties of the film, such as transmittance and reflectance, we average (5) over the film plane and introduce the effective film parameters u_e and v_e, by spatial averaging; thus,

$$u_e\langle \mathbf{E}\rangle = \langle u\mathbf{E}\rangle, \quad v_e\langle \mathbf{H}\rangle = \langle v\mathbf{H}\rangle. \tag{12}$$

Thereby, we obtain the relations

$$[\mathbf{n}\times(\langle \mathbf{E}_2\rangle - \langle \mathbf{E}_1\rangle)] = i v_e\langle \mathbf{H}\rangle, \quad [\mathbf{n}\times(\langle \mathbf{H}_2\rangle - \langle \mathbf{H}_1\rangle)] = -i u_e\langle \mathbf{E}\rangle, \tag{13}$$

which relate the spatially averaged fields on both sides of the film.

We suppose that the incident plane wave lies in the half-space $z < 0$, so that its electric field depends on z as $\exp(ik_0 z)$ (see Figure 1). The incident wave is partially reflected and partially transmitted through the film. The electric field amplitude in the half-space $z < 0$, away from the film, can be written as $\tilde{\mathbf{E}}_1(z) = \mathbf{E}_0\{\exp[ik_0(z + h/2 + a)] + r\exp[-ik_0(z + h/2 + a)]\}$, where r is the reflection coefficient and $\mathbf{E}_0$ is the amplitude of the incident wave. Well behind the film, the electric field acquires the form $\tilde{\mathbf{E}}_2(z) = t\exp[ik_0(z - h/2 - a)]$, where t is the transmission coefficient. In the reference planes $z = -h/2 - a$ and $z = h/2 + a$, the average electric field equals $\langle \mathbf{E}_1\rangle$ and $\langle \mathbf{E}_2\rangle$, respectively; therefore, $\langle \mathbf{E}_1\rangle = \tilde{\mathbf{E}}_1(-h/2 - a) = (1 + r)\mathbf{E}_0$ and $\langle \mathbf{E}_2\rangle = \tilde{\mathbf{E}}_2(h/2 + a) = t\mathbf{E}_0$. The same matching for the magnetic fields gives $\langle \mathbf{H}_1\rangle = (1 - r)[\mathbf{n}\times\mathbf{E}_0]$ and $\langle \mathbf{H}_2\rangle = t[\mathbf{n}\times\mathbf{E}_0]$. Substitution of these expressions for $\langle \mathbf{E}_{1,2}\rangle$ and $\langle \mathbf{H}_{1,2}\rangle$ in (6) and then in (13) gives two linear equations for t and r, whence

$$R \equiv |r|^2 = \left|\frac{(u_e - v_e)}{(i + u_e)(i + v_e)}\right|^2, \quad T \equiv |t|^2 = \left|\frac{1 + u_e v_e}{(i + u_e)(i + v_e)}\right|^2. \tag{14}$$

Thus, the effective ohmic parameters u_e and v_e completely determine the *observable* optical properties of inhomogeneous films.

Since the fields $\mathbf{E}(\mathbf{r})$ and $\mathbf{H}(\mathbf{r})$ are curl-free, they can be represented as gradients of certain scalar potentials as follows:

$$\mathbf{E} = -\nabla\varphi, \quad \mathbf{H} = -\nabla\psi. \tag{15}$$

By substituting these expressions, first in (9) and then in (8), we obtain the equations

$$\nabla\cdot[u(\mathbf{r})\nabla\varphi(\mathbf{r})] = 0, \quad \nabla\cdot[v(\mathbf{r})\nabla\psi(\mathbf{r})] = 0, \tag{16}$$

which are solved independently for the potentials φ and ψ. These equations are solved subject to the constraints

$$\langle -\nabla\varphi\rangle = \langle \mathbf{E}\rangle \equiv (1 + r + t)\mathbf{E}_0, \quad \langle -\nabla\psi\rangle = \langle \mathbf{H}\rangle \equiv (1 - r + t)[\mathbf{n}\times\mathbf{E}_0],$$

where the spatially uniform field $\mathbf{E}_0$ is the amplitude of the incident wave plane wave, and r and t are reflection and transmission coefficient, respectively.

The local electromagnetic fields obtained from the numerical solution of (16) are plotted in Figure 2 [35]. The maximums of the local fields are larger than the intensity of the incident plane wave by 4 to 5 orders of magnitude. The giant field fluctuations result in several new physical effects such as percolation-enhanced Rayleigh scattering, nonlinear scattering, percolation-enhanced Raman scattering, and huge enhancement of Kerr as well as other optical nonlinearities [1-2].

3 Surface plasmon polaritons

We consider now electromagnetic waves propagating on the surface of a metallic film. In the optical and infrared regimes, the collective excitation of the electron density (which is coupled to the near field) results in a surface plasmon polariton (SPP) (also known as a surface polariton [44-45]) traveling on the metal surface. These surface waves are excited when the real part of the metallic permittivity $\varepsilon_m = \varepsilon'_m + i\varepsilon''_m$ is negative (i.e., $\varepsilon'_m < 0$) and dissipation is small (i.e., $\kappa = \varepsilon''_m/|\varepsilon'_m| \ll 1$), which is typical for a metal in the optical regime. Let us denote $\varepsilon_m = -\nu^2$, where $\nu = -in$ is almost positive since the losses are small. At the metal–air interface, the SPP is an H wave, with its magnetic field parallel to the interface [45]. In the direction perpendicular to the interface, SPPs exponentially decay on both sides of the interface. The relation between the angular frequency ω and the wavenumber k_p of the SPP can be found from the following consideration.

We assume that the SPP propagates in the x direction, with $\mathbf{H}$ parallel to the y axis: $\mathbf{H} = \{0, H, 0\}$. The half-space $z > 0$ is vacuous while the metal fills the half-space $z < 0$. We seek solutions of the form

$$H_1 = H_0 \exp(ik_p x - \Lambda_1 z), \quad z > 0, \tag{17}$$

$$H_2 = H_0 \exp(ik_p x + \Lambda_2 z), \quad z < 0, \tag{18}$$

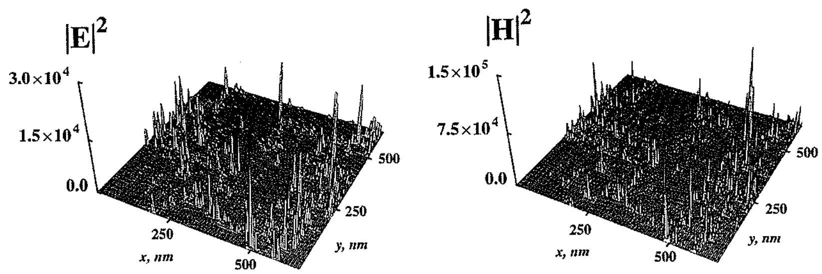

Figure 2 Distribution of local field intensities $|E|^2 = |E_1(\mathbf{r})|^2$ and $|H|^2 = |H_1(\mathbf{r})|^2$ in silver-dielectric percolation film for wavelength $\lambda_0 = 1$ μm and thickness $h = 50$ nm; concentration of silver particles is at the percolation threshold (silver surface concentration $p \approx 0.5$). Average field amplitudes are normalized to unit magnitude (i.e., $|\langle \mathbf{E}_1 \rangle| = |\langle \mathbf{H}_1 \rangle| = 1$).

where $\Lambda_1 = (k_p^2 - k_0^2)^{1/2}$ and $\Lambda_2 = [k_p^2 + (k_0 \nu)^2]^{1/2}$. Thus, the boundary condition on the continuity of the tangential component of the magnetic field is automatically satisfied. The continuity of the tangential component of the electric field results in the condition

$$\frac{\partial H_1}{\partial z} = -\frac{1}{\nu^2}\frac{\partial H_2}{\partial z} \tag{19}$$

for $z = 0$. This equation yields the dispersion equation

$$k_p = \frac{k_0 \nu}{\sqrt{\nu^2 - 1}} \tag{20}$$

for the SPP wavenumber k_p. SPP propagation on the metal surface then requires that $|\nu| > 1$.

There are two kinds of SPP modes in a metal film of finite thickness h, which correspond to symmetric and antisymmetric (with respect to reflection in the plane $z = 0$) oscillations of the electron density on both interfaces. Hereafter, it is supposed that $|\nu| > 1$. With the assumption of a strong skin effect, i.e., $\exp[-hk_0 \operatorname{Re}(\nu)] \ll 1$, the propagation of SPP is determined by the relation

$$k_{1,2} = k_p\left[1 \pm \frac{2\nu^2}{\nu^4 - 1}\exp(-hk_p\nu)\right], \tag{21}$$

where the wavenumbers k_1 and k_2 correspond to the symmetric and antisymmetric modes, respectively, and k_p is defined by (20). The phase velocities of the symmetric and antisymmetric SPPs are less than the speed of light c, and neither type can be excited by an external electromagnetic wave, because that would violate the principle of conservation of momentum. In a sense, the SPPs represent a *hidden reality* that is invisible, since an SPP does not interact with impinging light.

4 Resonant transmission

The situation changes dramatically when the metallic film is periodically inhomogeneous. The permittivity modulation provides the momentum needed to compensate for the difference between the momentums of the photon and the SPP. Hence, an SPP can be excited by an incident plane wave regardless of film thickness. An example of such spatial modulation is the square array of nanoholes punched into a metallic film [46]-[49]. Another example of a regular modulation of the refractive index, which we propose in Section 5, is light-induced modulation due to optical Kerr nonlinearity.

As before, a plane wave of interest is incident normally on the film. Then, the electromagnetic field inside the film is spatially modulated with the period L because of the film inhomogeneity, whether specially fabricated or light-induced. When the frequency of an incident wave is such that either of the SPP wavelengths

$\lambda_{1,2} = 2\pi/k_{1,2}$ coincides with L, the corresponding SPPs are excited in the film. If the film is optically thick, the SPP is excited initially on the front interface. Finally, it spreads out on *both* sides of the film.

There is a straightforward analogy between the front and back SPP components on the one hand and two identical oscillators coupled together on the other hand. The coupling can be arbitrarily weak; nevertheless, if we push the first oscillator, then after some time (which depends on the coupling) the second oscillator begins to oscillate with the same amplitude as the first oscillator. By the same token, the front and back SPP will eventually have the same amplitudes. When the SPP propagates on the back interface, it interacts with the permittivity modulation and, as a result, converts its energy back to a plane wave re-emitted from the film. Therefore, at resonance, the film becomes almost transparent, regardless of its thickness; however, the width of the transmittance resonance shrinks when the film thickness increases.

The amplitude $g \sim \Delta\varepsilon/\varepsilon$ of the permittivity modulation does not play any role in this scenario. Although g could be arbitrarily small, the front and back SPPs could be excited and the film would become transparent. Moreover, we do not need nanoholes through the film for resonant transmission to occur. All that is required is that both sides of the metal film are modulated with the same spatial period. The minimum g needed for resonant transmission depends on the loss in the metal; but the loss can be relatively small if the skin effect is strong. The transmittance maximum typically has a doublet structure corresponding to the excitation of symmetric and antisymmetric SPPs, as we show next.

A periodic modulation can always be represented by a Fourier series. Resonant transmission takes place when the wavelength of the impinged light is such that one of the SPP wavenumbers $k_{1,2}$ equals the wavenumber q of a spatial harmonic. The resonant interaction of an SPP with the qth spatial harmonic results in enhanced transmission. Since other spatial harmonics are nonresonant, we can consider light interaction with qth harmonic only. We suppose that magnetic field $\mathbf{H}$ in the wave normally impinging on the film has only a y component: $\mathbf{H} = \{0, H, 0\}$. We have to consider the interaction of the incident plane wave with a metal film whose permittivity varies as

$$\varepsilon(\mathbf{r}) = -\nu^2(1 + g\cos qx), \tag{22}$$

with $g \ll 1$.

The amplitude of a normally incident plane wave depends on z only. In the course of the interaction with the periodic permittivity (22), an electromagnetic harmonic varying as $\cos qx$ is generated. The amplitude of this harmonic is proportional to $g \ll 1$. This harmonic, in turn, interacts with the film modulation and thus generates a harmonic varying as $\cos 2qx$ and other higher harmonics. Thus, the whole spectrum of the electromagnetic wave is excited in the film when the incident plane wave interacts with the permittivity modulation. The amplitudes of the

$\cos pqx$ harmonics are proportional to g^p, $(p = 1, 2, 3, \ldots)$. Resonant transmission occurs when these harmonics are converted back to the plane wave transmitted through the film.

We are interested in the electromagnetic harmonics that can be converted back to the plane wave in such a way that this optical process is proportional to the lowest power of the modulation amplitude g. Therefore, we restrict our attention to the $\cos qx$ harmonic and write the magnetic field as $\tilde{H}(\mathbf{r}, z) = H(z) + H_q(z)\cos qx$, where $H(z)$ and $H_q(z)$ are two unknown functions. Substituting the field $\mathbf{H} = \{0, H(z) + H_q(z)\cos qx, 0\}$ in the Maxwell equations, equating the terms that have the same dependence on x [50], and neglecting the generation of higher harmonics, we obtain the system of two differential equations that determine the fields inside the film as follows:

$$\begin{aligned} &\frac{d^2}{dz^2}H(z) - (k_0\nu)^2 H - \frac{g}{2}\frac{d^2}{dz^2}H_q(z) = 0, \\ &\frac{d^2}{dz^2}H_q(z) - \left[(k_0\nu)^2 + q^2\right]H_q - g\frac{d^2}{dz^2}H(z) = 0. \end{aligned} \tag{23}$$

The transmitted magnetic field $H(z) = t\exp(ik_0 z)$, $(z > h/2)$, where $T = |t|^2$ is the transmittance. For the $\cos qx$ harmonic, we use the radiative boundary conditions; namely,

$$H_q(z) = \begin{cases} Y_3 \exp\left(-i\sqrt{k_0^2 - q^2}z\right), & z < -h/2 \\ Y_4 \exp\left(i\sqrt{k_0^2 - q^2}z\right), & z > h/2 \end{cases}, \tag{24}$$

where Y_3 and Y_4 are constants.

We neglect nonresonant (direct) transmittance, which allows us to obtain a rather simple expression for the resonant transmittance:

$$T(\tilde{\Delta}) = \frac{4\tilde{g}^4}{[(\tilde{\Delta} - 1)^2 + (\tilde{g}^2 + \tilde{\kappa})^2][(\tilde{\Delta}+1)^2 + (\tilde{g}^2 + \tilde{\kappa})^2]}. \tag{25}$$

This quantity depends on

$$\tilde{\Delta} = g^2 \frac{|\nu|(|\nu| - m)^2(|\nu| + |\nu|^3 + 2m)}{8(1 + |\nu|^2)\zeta} - \frac{\Delta}{\zeta}\frac{m(1 + |\nu|^2)}{2|\nu|}, \tag{26}$$

which is the normalized detuning from the SPP frequency; and it also depends on the renormalized modulation amplitude

$$\tilde{g} = \frac{g|\nu|\sqrt{m}(|\nu| - m)}{2\sqrt{1 + |\nu|^2}\sqrt{\zeta}} \tag{27}$$

as well as the renormalized loss factor

$$\tilde{\kappa} = \frac{(1 + |\nu|^2)\kappa}{4|\nu|^2\zeta}, \tag{28}$$

where $m = \sqrt{|\nu|^2 - 1}$, $\Delta = k_0/q - m/|\nu|$, and $\zeta = \exp(-h|\nu|q)$. Recall that we wrote $\varepsilon_m = -\nu^2$, and we also assumed small losses (i.e., $\kappa = \varepsilon''_m/|\varepsilon'_m| \ll 1$) and $|\nu| > 1$.

To analyze the resonant transmission, for simplicity, we set $\tilde{\kappa} = 0$ in (25). Then, for $\tilde{g} < 1$, it follows that $T(\tilde{\Delta})$ has two maximums; namely, $T(\tilde{\Delta}_1) = T(\tilde{\Delta}_2) = 1$ for $\tilde{\Delta}_{1,2} = \pm\sqrt{1 - \tilde{g}^4}$. Therefore, a lossless film becomes absolutely transparent at resonances, regardless of its thickness.

It is instructive to consider how the transmittance changes when $\tilde{g}$ increases. The distance between the two maximums, given by $\tilde{\Delta}_1 - \tilde{\Delta}_2 = 2\sqrt{1 - \tilde{g}^4}$, decreases with increasing $\tilde{g}$. The film remains transparent at both resonances. Finally, when $\tilde{g}$ exceeds unity, the two maximums merge together; and the transmission spectrum displays just one maximum, with transmittance $T_m = 4\tilde{g}^4/(1 + \tilde{g}^2)^2$ that decreases with further increase of $\tilde{g}$, as shown in Figure 3. The reason is that interaction with the permittivity modulation results in the radiative decay of the SPP and its conversion to the emitted plane wave. The radiative losses, conveyed by the $\tilde{g}^2$ term in the denominator of (25), lead to a damping of the SPP. As a result, resonant transmittance increases with a decreasing permittivity modulation $\tilde{g}$, and *vice versa*.

Resonant transmittance of a silver film is shown in Figure 4. The plot holds for $\kappa = 1.6 \times 10^{-3}$, which is realistic at cryogenic temperatures, when the electron mean-free path is determined by the film thickness h. Clearly, the transmittance has sharp two peaks corresponding to the SPP excitation, although the transmittance is less than 100% due to losses. Outside the resonance regime, the transmittance is estimated as $T \sim \exp(-2|\nu|k_0d) \sim 10^{-6}$. Thus, at resonance, the transmittance is enhanced by five orders of magnitude.

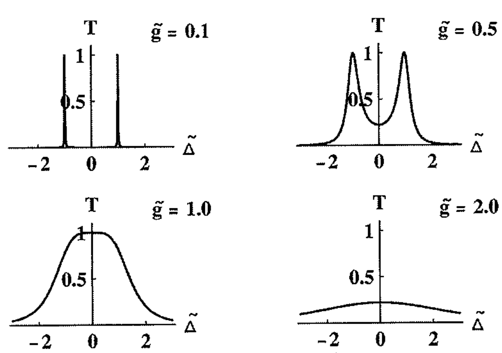

Figure 3 Transmittance as a function of normalized detuning $\tilde{\Delta}$ for different modulations $\tilde{g}$.

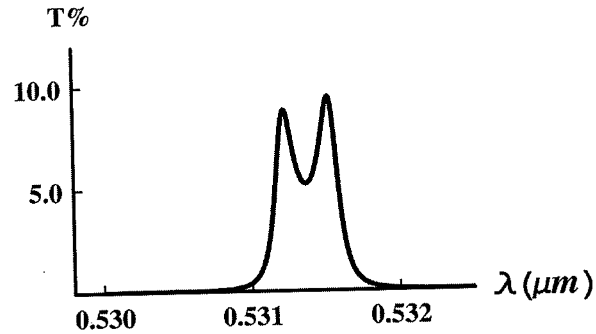

Figure 4 Transmittance of a silver film of thickness $d = 0.18$ μm, modulation $g = 0.1$, and spatial period $a = 2\pi/q = 0.5$ μm.

5 Light-induced resonant transmission

In Section 4, we assumed that the periodic permittivity modulation to be fabricated. Let us now consider the creation and control of this modulation by light itself through optical nonlinearity of the Kerr type [51]. We first suppose that film has a "seed" modulation $g_0 \ll 1$ and then determine the increase in g due to the film nonlinearity. Exactly at resonance, the transmitted intensity $I_t = T I_0$ is of the same order of magnitude as the intensity I_0 of the incident plane wave. The transmitted wave is generated by the SPP which propagates on the front interface $(z = -h/2)$ because of interaction with the permittivity modulation. Therefore, the intensity I_p of the SPP is estimated as $I_p \sim I_t/g^2 \sim I_0/g^2 \gg I_0$. At the back interface $(z = h/2)$, the SPP intensity is of the same order of magnitude. The electric field E_p of the SPP is spatially modulated with the resonance wavenumber k_p. Thus, the field-induced modulation of the permittivity is estimated via $g \sim 24\pi\chi^{(3)}|E_p|^2$, where $\chi^{(3)}$ is the nonlinear susceptibility quantifying the Kerr effect. The induced modulation of the permittivity increases the transmittance and, therefore, the intensity of the SPP. This positive feedback may result in the bistability depicted in Figure 5.

When dimensionless intensity of the impinging light I^* becomes larger than $I_1^* \simeq 6 \times 10^{-3}$, the transmittance T jumps from nearly zero to almost unity, and the film suddenly becomes transparent. If I^* is reduced thereafter, the film remains transparent even for $I^* < I_1^*$, since the SPP has been already excited in the film. Transmission declines steeply for $I^* \sim I_2^* \simeq 10^{-3} < I_1^*$. Thus, optical bistability can occur in periodically nonhomogeneous metallic films. The susceptibility $\chi^{(3)}$ is rather large for noble metals (typically, $\chi^{(3)} > 10^{-8}$ esu [52-53]), and the intensity I_0 required for the bistability can be easily achieved with conventional lasers. We also note that the seed modulation g_0 can be created by the interference of two additional control laser beams that are incident on the surface from the different sides with respect to the normal.

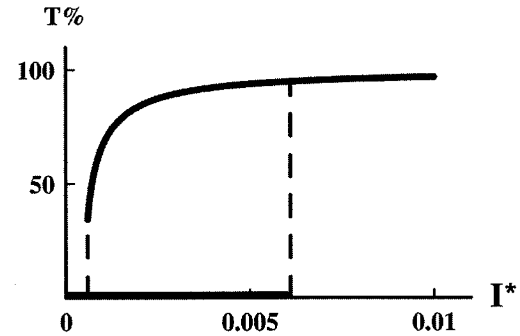

Figure 5 Nonlinear transmittance as a function of the intensity I_0 of the incident plane wave; $I^* = 24\pi^2 I_0 \chi^{(3)}/c$.

6 Extraordinary optical transmittance through nanoholes

Let us now apply the approach developed in Section 2.4 in order to investigate the interaction of light with nanoholes punched in an otherwise optically thick metal film. We show that the transmittance of a metal film with subwavelength-sized holes has sharp resonances corresponding to the excitation of the localized surface waves that are specific to a metal film with holes [54].

This extraordinary optical transmittance (EOT) phenomenon was discovered by Ebbesen *et al.* [46], who also subjected it to intensive examination; see also Sonnichsen *et al.* [55]. Various models—mostly numerical simulations—were suggested to explain the EOT [35], [49], [56]-[60]. Despite the very sophisticated simulation algorithms used, the physical nature of this phenomenon is not fully understood. Here we use a GOL approximation to develop a physical model that provides a simple qualitative picture.

Our objective is to find the transmittance of a metal film with subwavelength-sized holes. The local electric and magnetic fields, $\mathbf{E}(\mathbf{r})$ and $\mathbf{H}(\mathbf{r})$, can be determined from the potentials involved in (16); and then the effective parameters u_e and v_e can be obtained from the definitions (12). Since both $\mathbf{E}(\mathbf{r})$ and $\mathbf{H}(\mathbf{r})$ are curl-free, while both $\mathbf{D}(\mathbf{r})$ and $\mathbf{B}(\mathbf{r})$ are divergence-free, the quasi-static approximation can be used [1], [35]. Therefore, many efficient analytical and numerical methods, which were developed in quasi-static percolation theory, are at our disposal for the calculation of the local fields and the effective parameters [1], [4].

Here we use the simplest approximation—the Maxwell Garnett (MG) approach—that holds when the surface hole concentration p is small (i.e., $p \ll 1$). In two dimensions, the MG approach leads to the following expressions:

$$E_h = \frac{2u_m}{u_m + u_h} E_m, \quad H_h = \frac{2v_m}{v_m + v_h} H_m, \tag{29}$$

where u_m, v_m and v_h, v_h are the ohmic parameters for the metal and holes, E_m and H_m are electric and magnetic fields averaged over the metal, E_h and H_h are the fields averaged over the holes. From (12) and (29) we obtain the effective *electric* parameter:

$$u_e \equiv \frac{\langle uE \rangle}{\langle E \rangle} = \frac{(1-p)u_m E_m + p u_h E_h}{(1-p)E_m + pE_h}. \tag{30}$$

Repeating the same procedure, we find the effective *magnetic* parameter

$$v_e \equiv \frac{\langle vH \rangle}{\langle H \rangle} = \frac{(1-p)v_m H_m + p v_h H_h}{(1-p)H_m + pH_h}, \tag{31}$$

analogously.

Hereafter we consider films whose thickness h is much larger than the skin depth δ in bulk metal ($h \gg \delta = 1/\mathrm{Im}[n]k_0$). This case corresponds to most of the experiments with subwavelength holes reported so far. With the assumption of strong skin effect, (10) and (11) readily yield

$$u_m = -\cot(ak_0), \quad v_m = \tan(ak_0), \tag{32}$$

so that $u_m = -1/v_m$. We substitute the parameters u_e and v_e in (14) to obtain the transmittance

$$T = \frac{16p^2|u_m{}^2(1+u_h v_h)|^2}{|\Sigma_1 \Sigma_2|^2}, \tag{33}$$

where

$$\Sigma_1 = u_h - pu_h + (1+p)(1-iu_h)u_m - i(1-p)u_m^2 \tag{34}$$

and

$$\Sigma_2 = (i+u_m)(u_m v_h - 1) + p(i-u_m)(u_m v_h + 1). \tag{35}$$

In deriving (33), we assumed that (i) $p \ll 1$ and (ii) $|u_m| \gg 1$, which follows from (32) when the hole diameter $D \sim a \ll \lambda$.

The electric field E_h in a hole tends towards infinity in the limit $u_m \to -u_h$ if there are no losses; see (29). By utilizing the relation $u_m = -u_h$ in (33), we obtain transmittance $T = 4|u_m|/|1+u_m^2|$, which does not depend on the hole concentration p and, therefore, remains finite even as $p \to 0$. Similarly, when magnetic resonance takes place (i.e., $v_m = -1/u_m = -v_h$), the resonant transmittance also remains finite as $p \to 0$. Consequently, we conclude that the electric and magnetic resonances in the holes can result in EOT.

Note, however, that a strong electric field in a hole could excite an SPP that emerges from the hole. Then, the resonance would be damped due to radiative losses. As radiative losses are ignored in the following analysis, the expressions for the transmittance obtained in the remainder of this section should be considered as merely estimates.

7 Electric and magnetic resonances

To estimate the transmittance we should find ohmic parameters u_h and v_h for a hole. The parameters u_h, and v_h depend on the field distribution inside the hole. The internal field is a superposition of different eigenmodes for a subcritical waveguide that characterizes a hole. At the hole entrance, the internal field is similar to a plane wave, even though its amplitude can be significantly different from the amplitude of the incident wave. Deeper inside the hole, only the mode with the least eigenvalue survives. To simplify further semiquantitative analysis, we assume that the internal field is a plane wave near the entrance of the hole and it matches the fundamental internal mode at a distance a from both ends of the hole. We use for this matching the same distance a that we used earlier to match local fields with the incident plane wave. As a result, we obtain

$$u_h = v_h = \tan[(a + h/2)k_0] \tag{36}$$

for $h < 2a$, and

$$u_h = \frac{k_0 \tan(2ak_0) - \sqrt{\kappa^2 - k_0^2}\tanh[(h/2 - a)\sqrt{\kappa^2 - k_0^2}]}{k_0 + \sqrt{\kappa^2 - k_0^2}\tan(2ak_0)\,\tanh[(h/2 - a)\sqrt{\kappa^2 - k_0^2}]}, \tag{37}$$

$$v_h = \frac{\sqrt{\kappa^2 - k_0^2}\tan(2ak_0) + k_0 \tanh[(h/2 - a)\sqrt{\kappa^2 - k_0^2}]}{\sqrt{\kappa^2 - k_0^2} - k_0 \tan(2ak_0)\tanh[(h/2 - a)\sqrt{\kappa^2 - k_0^2}]} \tag{38}$$

for $h > 2a$. Here, $\kappa = 3.68/D$ is the eigenvalue for the basic mode in a cylindrical waveguide of diameter D [45, Ch. 92]. We denote the hole diameter and diameter of a metal particle (see Section 2) by the same symbol D, since in both cases D characterizes the typical size of an inhomogeneity.

Consider first shallow holes of depth $h < 2a$. By substituting (32) and (36) into (33) and invoking the limit $p \ll 1$, we obtain

$$T(k_0) = \sum_{j=1,2,3,\ldots} \frac{A_j(k_0)}{A_j(k_0) + (4a+h)^2(k_0 - k_j)^2}, \tag{39}$$

where

$$A_j(k_0) = 4p^2 \sin^4\left(\frac{2aj\pi}{4a+h}\right) \tag{40}$$

and

$$k_j = \frac{j\pi}{4a+h} - \frac{p}{4a+h}\sin\left(\frac{4aj\pi}{4a+h}\right). \tag{41}$$

Clearly, the transmittance in (39) is the sum of the resonances located at $k_0 = k_j$, as shown in Figure 6. The transmittance T is almost a periodic function of k_0 for $p \ll 1$, though the peak width depends on k_0. A peak can disappear when the corresponding numerator $A_j(k_j)$ in (39) vanishes. The odd-numbered resonances in (39) correspond to a high electric field, whereas the even-numbered resonances indicate a high magnetic field in the holes of the film. This classification is shown clearly in Figure 7.

For deep holes ($h > 2a$), we obtain the transmittance by substituting the ohmic parameters from (32) and (38) into (33). The transmittance T is plotted in Figure 8 as a function of Dk_0. It follows from this plot that the k_0-dependence of T can be rather peculiar when the thickness of the film increases: the peaks corresponding to high electric and high magnetic fields in the holes can move closer and even merge together.

With the assumption of losslessness, the magnitude of the electric or magnetic field in the holes tends toward infinity at a transmittance resonance. In any real film, however, the resonant fields must remain of finite magnitudes by virtue of losses. Impedance boundary conditions [45, Ch. 87] assist in the incorporation of losses in the foregoing analyses. The transmittance thus obtained for a square array

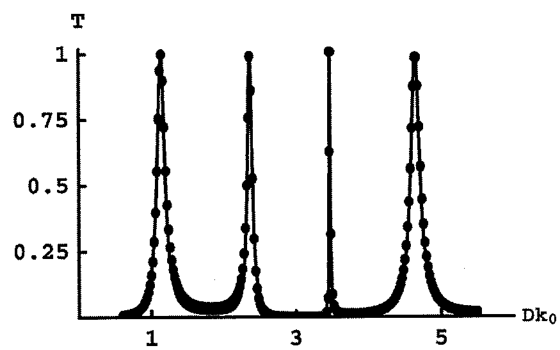

Figure 6 Transmittance through a metallic film with shallow holes ($h < 2a$); $a/D = 0.6$, $h/D = 0.8$, $p = 0.1$. The solid line is the resonance approximation (39), while the dots represent calculations with (33).

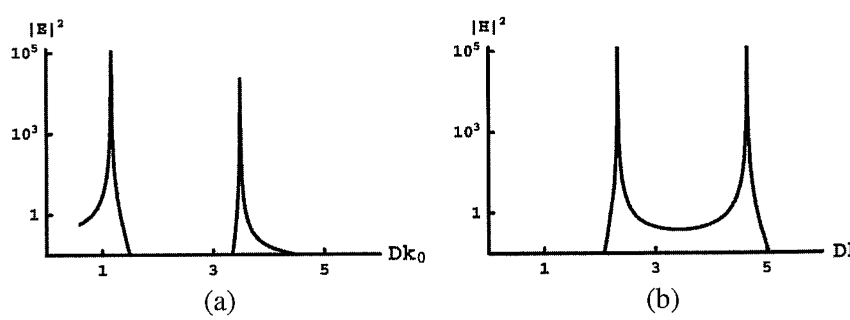

Figure 7 Magnitudes of the (a) electric field and (b) the magnetic field in a hole, when the incident field amplitude equals unity. See Figure 6 for the system parameters.

of nanoholes in a silver film is in qualitative agreement with experiments [46-47], [62], as illustrated in Figure 9. Most peaks in the transmittance are due to excitation of the SSP in the holes.

In calculating the transmittance presented in Figure 9, we also accounted for the SPP, which is not localized in a hole but propagates over the entire surface of the film. The propagating SPP is excited when the distance between adjacent holes coincides with $2\pi/k_{1,2}$ [see (20) and (21)]. This results in a peak at $\lambda_0 \simeq 0.6\ \mu$m in Figure 9(a), as well as for a small change in amplitude of the peak at $\lambda_0 \simeq 0.8\ \mu$m in Figure 9(b).

8 Light circuiting in nanoholes

We have considered so far the uniform illumination of the metal films by a plane wave. It is interesting to consider another possibility when only one of the holes

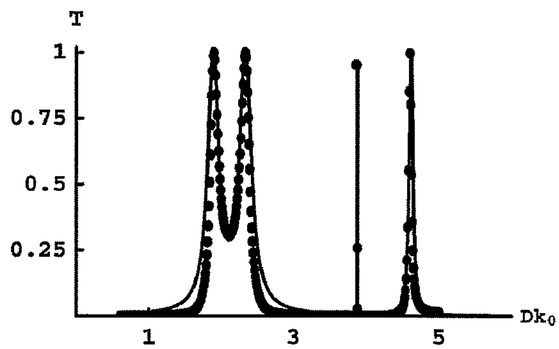

Figure 8 Transmittance through a film with deep holes $(h > 2a)$; $a/D = 0.6$, $h/D = 1.45$, $p = 0.1$.

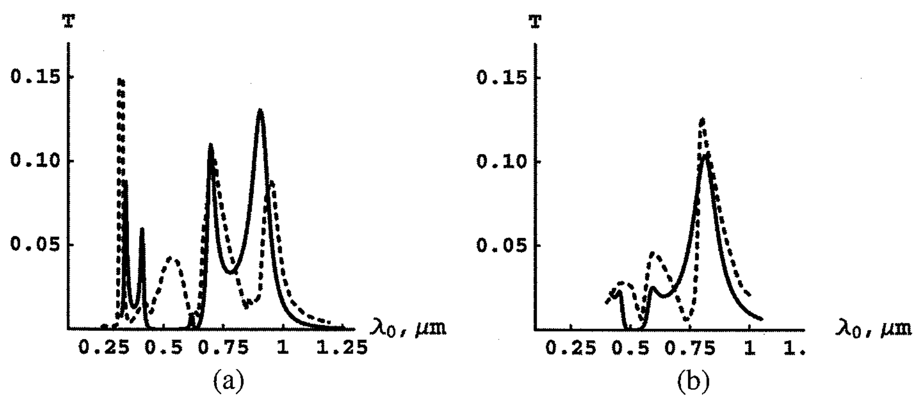

Figure 9 Figure 9: Extraordinary optical transmittance through a square array of nanoholes in (a) silver film on a quartz substrate ($D = 0.15\ \mu$m, $h = 0.2\ \mu$m, $p = 0.049$, $a/D = 0.6$), and (b) free-standing silver film ($D = 0.28\ \mu$m, $h = 0.32\ \mu$m, $p = 0.049$, $a/D = 0.6$). The dashed lines represent experimental data. The solid lines show theoretical results.

is illuminated by a nanosized light source. This can be accomplished, for example, with a nanometer-size probe of a near-field scanning optical microscope [61]. At resonance, the electric field (and/or the magnetic field) spreads out from the illuminated hole toward other holes, because of interactions between the holes via plasmons. Such holes can be arranged into any desired pattern to localize light and circuit the propagation of the electromagnetic energy, as shown in Figure 10. Thus, in Figures 10(c) and 10(d), we show how light circuiting depends on the polarization of the source. When the electric field, which excites the central hole, changes its polarization from parallel to "T" stem [Figure 10(c)] to perpendicular [Figure 10(d)], the light changes the direction of its propagation at a scale that is much smaller than the wavelength of the guided light.

9 Concluding remarks

The observable optical properties of thin metal-dielectric films were reviewed in this chapter. An approximation premised on the Generalized Ohm's Law (GOL) allows calculation of the field distributions in and the transmittances of inhomogeneous metal films. Computer simulations show giant electromagnetic field

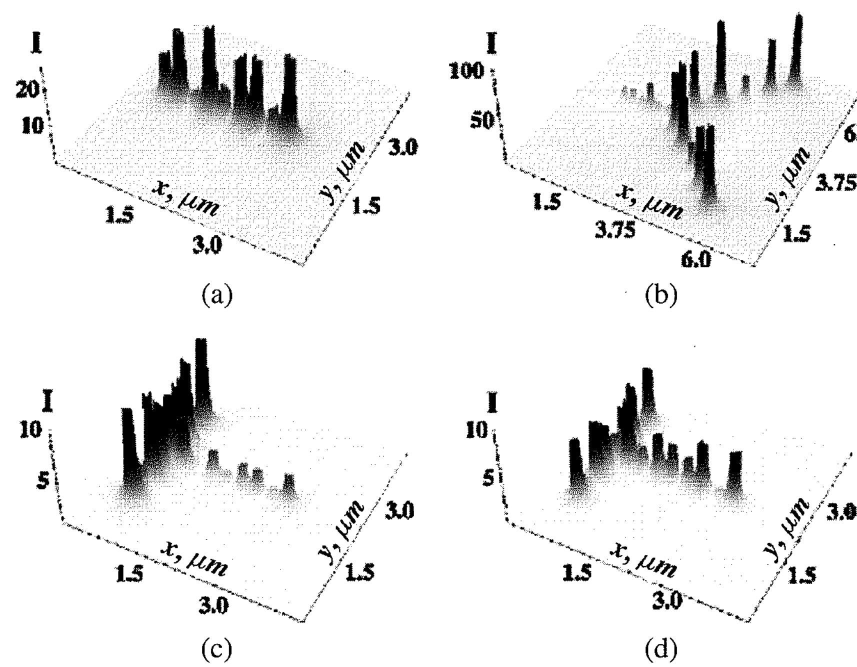

Figure 10 Nanocircuits formed by a pattern of nanoholes in a metallic film. (a) A line waveguide, wherein the first left hole is excited; (b) a fork waveguide, wherein first left hole is excited, (c) and (d) switch; center hole in top "T" is excited by electric field E: (c) $E \perp$ top T, (d) $E \parallel$ top T. Input parameters: $D = 0.15\ \mu$m, $h = 0.2\ \mu$m, $\lambda = 0.78\ \mu$m, and distance between the holes centers $= 0.3\ \mu$m.

fluctuations in such films. Indeed, giant electric field fluctuations near the percolation threshold in metal-dielectric films have already been observed in the microwave [22] and optical [32-33], [37-38] regimes. These fluctuations result in a huge enhancement of various optical effects. For example, surface enhancement for Raman scattering is proportional to the fourth moment of the field [24], [26], which is strongly enhanced. The same is valid for the Kerr nonlinearity, which is also proportional to the fourth moment [25], [31].

The excitation of a surface plasmon polariton (SPP) in periodically modulated metal films can result in resonant transmission, so that an optically thick film can become transparent. The transmittance can be increased by factors of $> 10^5$ at the resonance.

Resonant transmittance spectrums have a characteristic double-peak structure due to the splitting of SPPs into symmetric and antisymmetric modes. The resonance transmittance increases with decreasing losses in the system, which can be achieved by cooling the film to cryogenic temperatures. Exactly at the resonance, the amplitude of the excited SPP can be larger than the amplitude of the incident wave by several orders of magnitude. Then, optical nonlinearity can be significantly enhanced. We predicted that at sufficiently large intensities of the impinging light, the film can manifest the optical bistability, a phenomenon that can be exploited for optical switching.

Extraordinary light transmittance through optically thick metallic films with subwavelength-sized holes is possible. The transmittance has sharp resonances corresponding to the excitation of various surface waves. Some of these waves are similar to SPP, while others are localized surface waves that are specific for a perforated metal and have not been discussed elsewhere. Nanoholes can be arranged into any desired pattern to localize and circuit em energy. Such nanoengineered structures could be used as integrated elements in various optoelectronic and photonic devices, including most sophisticated ones such as optical computers.

Acknowledgment

The authors are grateful to Academician A.M. Dykhne and Dr. V. Podolskiy for useful discussions. This work was supported by Battelle (DAAD19-02-D-0001), NASA (NCC-1-01049), ARO (DAAD19-01-1-0682), and NSF (ESC-0210445).

References

[1] A.K. Sarychev and V.M. Shalaev, Electromagnetic field fluctuations and optical nonlinearities in metal-dielectric composites, *Phys Rept* **335** (2000), 275–371.

[2] A.K. Sarychev and V.M. Shalaev, Field distribution, Anderson localization, and optical phenomena in random metal-dielectric films, *Optics of nanostructured materials* (V.A. Markel and T. George, eds), Wiley, New York, NY, USA, 2000.

[3] V.M. Shalaev, *Nonlinear optics of random media: Fractal composites and metal-dielectric films*, Springer, Heidelberg, Germany, 2000.

[4] D.J. Bergman and D. Stroud, Physical properties of macroscopically inhomogeneous media, *Solid State Phys* **46** (1992), 147–269.

[5] J.P. Clerc, G. Giraud, J.M. Laugier and J.M. Luck, The AC electrical-conductivity of binary disordered-systems, percolation clusters, fractals and related models, *Adv Phys* **39** (1990), 191–308.

[6] R.W. Cohen, G.D. Cody, M.D. Coutts and B. Abeles, Optical properties of granular silver and gold films, *Phys Rev B* **8** (1973), 3689–3701.

[7] G.A. Niklasson and C.G. Granqvist, Optical-properties and solar selectivity of coevaporated Co-Al_2O_3 composite films, *J Appl Phys* **55** (1984), 3382–3410.

[8] L.C. Botten and R.C. McPhedran, Phase constraints for lossy symmetric structures, *Optica Acta* **32** (1985), 595–605.

[9] M. Gajdardziska-Josifovska, R.C. McPhedran, D.R. McKenzie and R.E. Collins, Silver magnesium fluoride cermet films. Optical and electrical-properties, *Appl Opt* **28** (1989), 2744–2753.

[10] C.A. Davis, D.R. McKenzie and R.C. McPhedran, Optical-properties and microstructure of thin silver films, *Opt Commun* **85** (1991), 70–82.

[11] P. Gadenne, A. Beghadi and J. Lafait, Optical crossover analysis of granular gold-films at percolation, *Opt Commun* **65** (1988), 17–21.

[12] P. Gadenne, Y. Yagil and G. Deutscher, Transmittance and reflectance insitu measurements of semicontinuous gold-films during deposition, *J Appl Phys* **66** (1989) 3019–3025.

[13] Y. Yagil, M. Yosefin, D.J. Bergman, G. Deutscher and P. Gadenne, Scaling theory for the optical-properties of semicontinuous metal-films, *Phys Rev B* **43** (1991), 11342–11352.

[14] Y. Yagil, P. Gadenne, C. Julien and G. Deutscher, Optical-properties of thin semicontinuous gold-films over a wavelength range of 2.5 to 500 μm, *Phys Rev B* **46** (1992), 2503–2511.

[15] T.W. Noh, P.H. Song, Sung-Il Lee, D.C. Harris, J.R. Gaines and J.C. Garland, Far-infrared studies of 2-dimensional random metal-insulator composites, *Phys Rev B* **46** (1992), 4212–4221.

[16] A.K. Sarychev, D.J. Bergman and Y. Yagil, Optical and microwave properties of metal-insulator thin films: possibility of light localization, *Physica A* **207** (1994), 372–378.

[17] A.K. Sarychev, D.J. Bergman and Y. Yagil, Theory of the optical and microwave properties of metal-dielectric films, *Phys Rev B* **51** (1995), 5366–5385.

[18] R. Levy-Nathansohn and D.J. Bergman, Studies of the generalized Ohm's law, *Physica A* **241** (1997), 166–172.

[19] R. Levy-Nathansohn and D.J. Bergman, Decoupling and testing of the generalized Ohm's law, *Phys Rev B* **55** (1997), 5425–5439.

[20] S. Blacher, F. Brouers and A.K. Sarychev, Multifractality of giant electric field fluctuations in semicontinuous films, *Fractals in the natural and applied sciences* (M.M. Novak, ed), Chapman and Hall, London, UK, 1995.

[21] E.M. Baskin, M.V. Entin, A.K. Sarychev and A.A. Snarskii, Enhancement of high-frequency field in near-ideal metal mixture, *Physica A* **242** (1997), 49–56.

[22] A.N. Lagarkov, K.N. Rozanov, A.K. Sarychev and A.N. Simonov, Experimental and theoretical-study of metal-dielectric percolating films at microwaves, *Physica A* **241** (1997), 199–206.

[23] F. Brouers, A.K. Sarychev, S. Blacher and O. Lothaire, Giant field fluctuations and characteristic lengths in optical-properties of nano metal-dielectric films, *Physica A* **241** (1997), 146–153.

[24] F. Brouers, S. Blacher, A.N. Lagarkov, A.K. Sarychev, P. Gadenne and V.M. Shalaev, Theory of giant Raman scattering from semicontinuous metal films, *Phys Rev B* **55** (1997), 13234–13245.

[25] V.M. Shalaev and A.K. Sarychev, Nonlinear optics of random metal-dielectric films, *Phys Rev B* **57** (1998), 13265–13288.

[26] P. Gadenne, F. Brouers, V.M. Shalaev and A.K. Sarychev, Giant stokes fields on semicontinuous metal films, *J Opt Soc Am B* **15** (1998), 68–72.

[27] V.M. Shalaev, E.Y. Poliakov, V.A. Markel, V.P. Safonov and A.K. Sarychev, Surface-enhanced optical nonlinearities of nanostructured fractal materials, *Fractals* **5** (1997), 63–82.

[28] V.M. Shalaev, V.A. Markel, E.Y. Poliakov, R.L. Armstrong, V.P. Safonov and A.K. Sarychev, Nonlinear Optical Phenomena in Nanostructured Fractal Materials, *J Nonlin Opt Phys Mat* **7** (1998), 131–152.

[29] F. Brouers, S. Blacher and A.K. Sarychev, Giant field fluctuations and anomalous scattering in semicontinuous metal films, *Phys Rev B* **58** (1998), 15897–15903.

[30] A.K. Sarychev, V.A. Shubin and V.M. Shalaev, Percolation-enhanced nonlinear scattering from metal-dielectric composites, *Phys Rev E* **59** (1999), 7239–7242.

[31] A.K. Sarychev, V.A. Shubin and V.M. Shalaev, Anderson localization of surface plasmons and nonlinear optics of metal-dielectric composites, *Phys Rev B* **60** (1999), 16389–16408.

[32] S. Grésillon, L. Aigouy, A.C. Boccara, J.C. Rivoal, X. Quelin, C. Desmarest, P. Gadenne, V.A. Shubin, A.K. Sarychev and V.M. Shalaev, Experimental observation of localized optical excitations in random metal-dielectric films, *Phys Rev Lett* **82** (1999), 4520–4523.

[33] S. Grésillon, J.C. Rivoal, P. Gadenne, X. Quelin, V.M. Shalaev and A.K. Sarychev, Nanoscale observation of enhanced electromagnetic field, *Phys Stat Sol (a)* **175** (1999), 337–346.

[34] A.K. Sarychev, V.A. Shubin and V.M. Shalaev, Giant high-order field moments in metal-dielectric composites, *Physica A* **266** (1999), 115–122.

[35] V.A. Shubin, A.K. Sarychev, J.P. Clerc and V.M. Shalaev, Local electric and magnetic fields in semicontinuous metal films: Beyond the quasistatic approximation, *Phys Rev B* **62** (2000), 11230–11244.

[36] M.I. Stockman, S.V. Faleev and D.J. Bergman, Localization versus delocalization of surface plasmons in nanosystems: Can one state have both characteristics? *Phys Rev Lett* **87** (2001), 167401.

[37] M. Breit, V.A. Podolskiy, S. Gresillon, G. von Plessen, J. Feldmann, J.C. Rivoal, P. Gadenne, A.K. Sarychev and V.M. Shalaev, Experimental observation of percolation-enhanced nonlinear light scattering from semicontinuous metal films, *Phys Rev* B **64** (2001), 125106.

[38] K. Seal, M.A. Nelson, Z.C. Ying, D.A. Genov, A.K. Sarychev and V.M. Shalaev, Growth, morphology, and optical and electrical properties of semicontinuous metallic films, *Phys Rev B* **67** (2003), 035318.

[39] A. Lakhtakia (ed), *Selected papers on linear optical composite materials*, SPIE Press, Bellingham, WA, USA, 1996.

[40] G.B. Smith, Nanostructured thin films, *Introduction to complex mediums for optics and electromagnetics* (W.S. Weiglhofer and A. Lakhtakia, eds), SPIE Press, Bellingham, WA, USA, 2003.

[41] T.G. Mackay, Homogenization of linear and nonlinear complex composite materials, *Introduction to complex mediums for optics and electromagnetics* (W.S. Weiglhofer and A. Lakhtakia, eds), SPIE Press, Bellingham, WA, USA, 2003.

[42] H.A. Bethe, Theory of diffraction by small holes, *Phys Rev* **66** (1944), 163–182.

[43] W.S. Weiglhofer, Constitutive characterization of simple and complex mediums, *Introduction to complex mediums for optics and electromagnetics* (W.S. Weiglhofer and A. Lakhtakia, eds), SPIE Press, Bellingham, WA, USA, 2003.

[44] V.D. Freilikher, E. Kanzieper and A.A. Maradudin, Coherent scattering enhancement in systems bounded by rough surfaces, *Phys Rept* **288** (1997), 127–204.

[45] L.D. Landau, E.M. Lifshitz and L.P. Pitaevskii, *Electrodynamics of continuous media, 2nd ed*, Pergamon Press, Oxford, UK, 1984.

[46] T.W. Ebbesen, H.J. Lezec, H.F. Ghaemi, T. Thio and P.A. Wolff, Extraordinary optical transmission through sub-wavelength hole arrays, *Nature* **391** (1998), 667–669.

[47] H.F. Ghaemi, T. Thio, D.E. Grupp, T.W. Ebbesen and H.J. Lezec, Surface plasmons enhance optical transmission through subwavelength holes, *Phys Rev B* **58** (1998), 6779–6782.

[48] T.J. Kim, T. Thio, T.W. Ebbesen, D.E. Grupp and H.J. Lezec, Control of optical transmission through metals perforated with subwavelength hole arrays, *Opt Lett* **24** (1999), 256–258.

[49] L. Martin-Moreno, F.J. Garcia-Vidal, H.J. Lezec, K.M. Pellerin, T. Thio, J.B. Pendry and T.W. Ebbesen, Theory of extraordinary optical transmission through subwavelength hole arrays, *Phys Rev Lett* **86** (2001), 1114–1117.

[50] Lord Rayleigh, *The theory of sound, 2nd ed*, Macmillan, London, UK, 1896.
[51] H.E. Brandt (ed), *Selected papers on nonlinear optics*, SPIE Press, Bellingham, WA, USA, 1991.
[52] S. Debrus, J. Lafait, M. May, N. Pincon, D. Prot, C. Sella and J. Venturini, Z-scan determination of the third-order optical nonlinearity of gold: silica nanocomposites, *J Appl Phys* **88** (2000), 4469–4475.
[53] P.J. Bennett, V. Albanis, Y.P. Svirko and N.I. Zheludev, Femtosecond cubic optical nonlinearity of thin nickel films, *Opt Lett* **24** (1999),1373–1375.
[54] A.K. Sarychev, V.A. Podolskiy, A.M. Dykhne and V.M. Shalaev, Resonance transmittance through a metal film with subwavelength holes, *IEEE J Quant Electron* **38** (2002), 956–963.
[55] C. Sonnichsen, A.C. Duch, G. Steininger, M. Koch, G. von Plessen and J. Feldmann, Launching surface plasmons into nanoholes in metal films, *Appl Phys Lett* **76** (2000), 140–142.
[56] W.C. Tan, T.W. Preist, R.J. Sambles and N.P. Wanstall, Flat surface-plasmon-polariton bands and resonant optical absorption on short-pitch metal gratings, *Phys Rev B* **59** (1999), 12661–12666.
[57] W.C. Tan, T.W. Preist and R.J. Sambles, Resonant tunneling of light through thin metal films via strongly localized surface plasmons, *Phys Rev B* **62** (2000), 11134–11138.
[58] L. Salomon, F.D. Grillot, A.V. Zayats and F. de Fornel, Near-field distribution of optical transmission of periodic subwavelength holes in a metal film, *Phys Rev Lett* **86** (2001), 1110–1113.
[59] R. Wannemacher, Plasmon-supported transmission of light through nanometric holes in metallic thin films, *Opt Comm* **195** (2001), 107–118.
[60] Q. Cao and P. Lalanne, Negative role of surface plasmons in the transmission of metallic gratings with very narrow slits, *Phys Rev Lett* **88** (2002), 057403.
[61] F. de Fornel, *Evanescent waves: From Newtonian optics to atomic optics*, Springer, Heidelberg, Germany, 2001.
[62] D.E. Grupp, H.J. Lezec, T.W. Ebbesen, K.M. Pellerin and T. Thio, Crucial role of metal surface in enhanced transmission through subwavelength apertures, *Appl Phys Lett* **77** (2000), 1569–1571.

Andrey K. Sarychev is a Senior Research Scientist in the School of Electrical and Computer Engineering at Purdue University. He obtained his Ph.D. in Physics and Mathematics in 1979 from Moscow Institute of Physics and Technology. In 1990, he was decorated with the Medal of Honor for his investigations of microwave composite materials. In 1993, he was awarded the degree of Doctor of Science from Russian Academy of Science; in 2000, he was nominated for member of the Academy. A.K. Sarychev has worked as a Visiting Professor in Tel Aviv University, Liege University, and the University of Provence in 1991–1995. During 1995–1998, he was head of the Theoretical Department at Institute of Theoretical and Applied Electrodynamics Russian Academy of Science. During 1998–2001, he was College Professor in the Physics Department at New Mexico State University. He has served as a Member of Program Committees for international conferences and presented numerous invited talks. Dr. Sarychev has authored 2 books and 4 book chapters, more than 100 original papers, and holds 5 patents. His current research interests include new optical and microwave materials and nanophotonics.

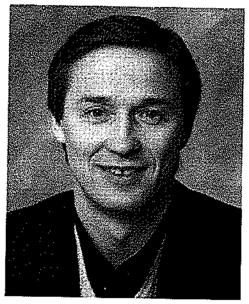

Vladimir M. Shalaev is a Professor of the School of Electrical and Computer Engineering at Purdue University. He is a Fellow of the American Physical Society and a Fellow of the Optical Society of America. Dr. Shalaev received his Ph.D. degree in Physics and Mathematics from University of Krasnoyarsk, Russia in 1983, where he then held an Assistant Professor position. In 1990 he was awarded the International Humboldt Fellowship and worked at University of Heidelberg, Germany, and University of Paris-Sud, France. In 1991–1993, he worked as a Research Professor at University of Toronto and Ontario Laser and Lightwave Center, Canada. From 1993 to 1997 he was Associate Professor and, from 1997 to 2001, Professor of Physics at New Mexico State University (NMSU). Since 1997 he has been George W. Gardiner Professor of Physics at NMSU. He has served as a Chair and Member of Program Committees for numerous international conferences and held invited professorships in several leading universities in France, Hong Kong, and Germany. Since 2001 he has been a Professor of Electrical and Computer Engineering at Purdue University. Dr. Shalaev has authored 2 books and 10 book chapters, nearly 200 technical papers and conference presentations (50 invited), and edited 2 books. His current research interests include nanophotonics and optical nanomaterials.